

## Sensitivity analysis of a pulse nutrient addition technique for estimating nutrient uptake in large streams

Laurence Lin\* and J. R. Webster

Department of Biological Sciences, Virginia Polytechnic Institute and State University

### Abstract

The constant nutrient addition technique has been used extensively to measure nutrient uptake in streams. However, this technique is impractical for large streams, and the pulse nutrient addition (PNA) has been suggested as an alternative. We developed a computer model to simulate Monod kinetics nutrient uptake in large rivers and used this model to evaluate the sensitivity of the PNA technique. We parameterize our model using the average hydrogeomorphological estimates from a pulse release study of ammonium in the Snake River, WY, and used this study to demonstrate how data from a field experiment can be effectively analyzed using a simulation model. To evaluate the sensitivity of the PNA technique, we manipulated the hydrogeomorphology and uptake kinetics of our stream model, simulated a pulse ammonium addition, and measured the downstream response in our model as if it were a field experiment, while ammonium areal uptake at ambient concentration was kept unchanged in the model. Ammonium uptake estimates by the PNA technique were different from the uptake in our model and these differences were nonrandom. The difference was greatest when velocity was high and there was little solute spread, either in the water column or from exchange with transient storage. The difference was also high when the half saturation coefficient for uptake was low. Our estimates of ammonium uptake under the assumption of Monod kinetics were higher than those under the assumption of first-order kinetics based on direct calculation from the experimental data.

Biological nutrient use is a key component of nutrient spiraling (Webster and Patten 1979; Newbold et al. 1981, 1982) in streams (e.g., Elwood et al. 1981; Rosemond et al. 1993; Martin et al. 2001). In nutrient spiraling, stream organisms take up nutrients from the water column and use these nutrients for production. Uptake length ( $S_w$ ) is the estimated distance a nutrient molecule travels in the water column before it is used by biotic or abiotic processes (Newbold et al. 1981; Webster and Valett 2006). It is also a measure of nutrient use efficiency in streams (Mulholland et al. 2002). In most stream nutrient studies, biological uptake within a reach has been assumed to be linearly proportional to the nutrient concentration in the water column (first-order kinetics) regardless of any abiotic and biotic factors that may change the relationship (Dodds et al. 2002; Kemp and Dodds 2002; Earl et al. 2006). Another way to model nutrient uptake flux and nutri-

ent concentration is to use Monod kinetics (Michaelis-Menten function, non-linear) (e.g., Bothwell 1989; Dodds et al. 2002; Mulholland et al. 2002; Claessens and Tague 2009) in which the nutrient supply has a saturation effect on biological uptake. Although Monod kinetics is a logical choice to represent the uptake process, its parameters (maximum uptake and half-saturation coefficient) are difficult to measure in streams because they require a series of nutrient addition experiments.

For the constant nutrient addition technique, the nutrient concentration is elevated above the ambient nutrient concentration for several hours over an entire reach. Mulholland et al. (2002) showed that the uptake length at an elevated nutrient concentration overestimated the “true” uptake length at ambient nutrient concentration. This is because biotic uptake does not increase linearly with nutrient concentration but rather increases asymptotically, consistent with a model such as the Monod model for nutrient kinetics. However, uptake lengths at different elevated nutrient concentrations can be used to calculate the “true” uptake length at ambient concentration using the technique developed by Payn et al. (2005).

In large river systems, the constant nutrient addition technique is impractical due to the large amount of nutrient required to elevate nutrient concentration in an entire reach (Tank et al. 2008). Therefore, a pulse nutrient addition tech-

\*Corresponding author: E-mail: lauren@vt.edu

### Acknowledgments

We thank Jennifer L. Tank for providing data and information for this study and Robert L. Runkel and Robert A. Payn for constructive suggestions. We also thank Dr. Luc Claessens for guidance during this study.

DOI 10.4319/lom.2012.10.718

nique (PNA technique) was suggested as an alternative for uptake measurement in large streams. This technique was first used by Meals et al. (1999) and more recently used to estimate nutrient uptake parameters by Tank et al. (2008) and Powers et al. (2009). Using the PNA technique, a slug of nutrient and biological conservative tracer is released, and their concentrations are monitored at several downstream stations. To measure nutrient uptake, Tank et al. (2008) (TPNA technique) calculated the total mass of nutrient and conservative tracer at each station by time integration. The logarithmic change in the ratio of nutrient mass to conservative tracer mass over downstream distance represented the longitudinal uptake rate. In the constant nutrient addition technique, the addition can be kept very small to minimize saturation effects. However, the PNA technique requires a relatively large but short-term nutrient elevation and sometimes leads to large enrichment relative to ambient conditions. Although the limitations of the PNA technique may be understood conceptually, the quantitative impacts of different hydrogeomorphology and different uptake saturation levels on the PNA technique have not been documented.

In this study, our objectives were (1) to develop a computer model to simulate nutrient uptake in a large river and quantitatively evaluate the sensitivity of the TPNA technique to different hydrogeomorphology and uptake saturation levels; and (2) to demonstrate how data from a field PNA experiment can be effectively analyzed to estimate nutrient uptake using a simulation model. We parameterize our model using the average hydrogeomorphological estimates of the Snake River, WY (Tank et al. 2008).

## Materials and procedures

### Model development

We began with the basic model of advection and longitudinal dispersion, including inflow, transient storage, and nutrient uptake in the water column and transient storage (e.g., Bencala and Walters 1983; Runkel 1998), but we did not include lateral inflow as the data of Tank et al. (2008) did not indicate a downstream increase in discharge:

$$\frac{\partial C}{\partial t} = -\frac{Q}{A} \frac{\partial C}{\partial x} + \frac{1}{A} \frac{\partial}{\partial x} \left( AD \frac{\partial C}{\partial x} \right) + \alpha(C - C_s) - U_c + M_c \quad (1)$$

$$\frac{\partial C_s}{\partial t} = -\frac{A}{A_s} \alpha(C - C_s) - U_s + M_s \quad (2)$$

$C$  is nutrient concentration in the water column,  $C_s$  is nutrient concentration in transient storage,  $Q$  is discharge,  $D$  is the longitudinal dispersion coefficient, and  $\alpha$  is the exchange rate between transient storage and water column.  $A$  is channel cross-sectional area,  $A_s$  is cross-sectional area of transient storage, and  $U_c$  and  $U_s$  are nutrient uptake fluxes in the stream channel and transient storage.  $M_c$  and  $M_s$  are nutrient mineralization fluxes in the stream channel and transient storage. In our model, these mineralization fluxes were equal

to nutrient uptake ( $U_c$  and  $U_s$ ) at the ambient nutrient level and remained constant throughout the simulations.

We kept discharge ( $Q$ ) and channel cross sectional area ( $A$ ) constant within a reach. Biotic nutrient uptake fluxes were simulated using Monod kinetics functions:

$$U_c = \frac{1}{z} \frac{CU_{cmax}}{k_{c1/2} + C} \quad \text{and} \quad (3)$$

$$U_s = \frac{CU_{smax}}{k_{s1/2} + C}$$

$U_{cmax}$  is the maximum nutrient areal uptake flux ( $\mu\text{g N m}^{-2} \text{s}^{-1}$ ) in the stream channel and  $U_{smax}$  is the maximum nutrient uptake flux ( $\mu\text{g N m}^{-3} \text{s}^{-1}$ ) in transient storage,  $k_{c1/2}$  and  $k_{s1/2}$  are the half-saturation coefficients for nutrient uptake in the stream channel and transient storage, and  $z$  is water depth.

### Model parameters for sensitivity analysis

Model parameters for both sensitivity analysis and uptake estimation were based on the study of the Snake River by Tank et al. (2008) (Tables 1 and 2). Tank et al. (2008) studied a 2610 m reach with an average channel width of 41 m, depth of 0.49 m, and discharge of 8.4  $\text{m}^3/\text{s}$  (based on morphology and salt travel time). They added 276 kg Cl (as NaCl) and 5.7 kg N (as  $[\text{NH}_4]_2\text{SO}_4$ ) to the river in a few seconds (3-5). We adapted the chloride data of Tank et al. (2008) into the OTIS-P model (Runkel 1998) and estimated hydrogeomorphological parameters for our simulated river in the sensitivity analysis. Specifically, we divided the reach into the four sub-reaches between sampling stations because we were unable to estimate reasonable values using the whole reach due to spatial variability within the reach. We then used the sub-reach length-weighted average for our sensitivity analysis ( $D = 0.01 \text{ m}^2 \text{ s}^{-1}$ ,  $A_c = 7.7 \text{ m}^2$ ,  $A_c/(A + A_s) = 0.26$ , and  $\alpha = 0.0024 \text{ s}^{-1}$ ) (Table 1).

Tank et al. (2008) estimated a longitudinal ammonium uptake rate ( $k_x$ ) of  $0.0005 \text{ m}^{-1}$ , corresponding to an uptake length of 2000 m and areal uptake flux ( $U$ ) of  $0.51 \mu\text{g N m}^{-2} \text{ s}^{-1}$  (based on average width, discharge, and ambient ammonium concentration). In our sensitivity analysis, we used these ammonium uptake estimates as the ambient nutrient uptake in the stimulated river at the ambient nutrient concentration ( $5 \mu\text{g NH}_4\text{-N L}^{-1}$ ) and at an average velocity of  $0.419 \text{ m s}^{-1}$  (based on salt travel time). Throughout the manuscript, we use "ambient uptake" to refer to these values.

For our first four sensitivity analyses (Monod kinetics uptake parameters, velocity, cross-sectional area, and channel-storage exchange rate), we assumed that 1) nutrient uptake in the river was solely in the stream channel or solely in transient storage and 2) at the ambient nutrient concentration ( $C_0$ ) Monod kinetics uptake in the stream channel or in transient storage was equal to the total areal uptake flux ( $U = 0.51 \mu\text{g N m}^{-2} \text{ s}^{-1}$ ) in the stream channel so that

**Table 1.** Model parameters for sensitivity analysis. The nominal value of each parameter was used when the parameter was not manipulated.

|   | Nominal value | Min value | Max value |
|---|---------------|-----------|-----------|
| Reach length (m)  | 2610          | —         | —         |
| Velocity ( $v$ , m s <sup>-1</sup> )  | 0.419*        | 0.4       | 1.4       |
| Cross-section area ( $A$ , m <sup>2</sup> )                                   | 20.01*        | 5.99†     | 20.97†    |
| Dispersion ( $D$ , m <sup>2</sup> s <sup>-1</sup> )                           | 0.01‡         | —         | —         |
| Cross section area of transient storage ( $A_s$ , m <sup>2</sup> )            | 7.70‡         | 2.0       | 40.00     |
| Transient storage exchange rate ( $\alpha$ , s <sup>-1</sup> )                | 0.0024‡       | 0.0002    | 0.003     |
| Uptake half-saturation constant ( $k_{1/2}$ , µg N L <sup>-1</sup> )          | 15            | 5         | 50        |
| Maximum areal uptake ( $U_{max}$ , µg N m <sup>-2</sup> s <sup>-1</sup> )     | 2.05          | 1.02      | 5.63      |
| Nutrient areal uptake ( $U$ , µg N m <sup>-2</sup> s <sup>-1</sup> ) at $C_0$ | 0.51          | —         | —         |

\*Velocity was determined as 2610 m divided by CI travel time, 103.8 min. Cross-section area was the product of 41 m width and 0.488 m depth.

†Cross-section area was modified as velocity changed from 0.4 to 1.4 m s<sup>-1</sup>, keeping discharge unchanged.

‡Averages are weighted based on sub-reach length.

**Table 2.** Model parameters. Averages are weighted based on sub-reach length.

|   | Full reach | Sub-reach 1 | Sub-reach 2 | Sub-reach 3 | Sub-reach 4 | Average of sub-reaches |
|---|------------|-------------|-------------|-------------|-------------|------------------------|
| Reach length (m)  | 2610       | 1330        | 100         | 320         | 860         | —                      |
| Velocity* ( $v$ , m s <sup>-1</sup> )   | 0.419†     | 1.26        | 0.05        | 0.22        | 0.38        | 0.79                   |
| Cross-section area* ( $A$ , m <sup>2</sup> )  | 20.01†     | 6.67        | 161.15      | 37.66       | 22.32       | 21.54                  |
| Dispersion* ( $D$ , m s <sup>-2</sup> )   | —          | 0.01        | 0.01        | 0.01        | 0.01        | 0.01                   |
| Cross section area of transient storage* ( $A_s$ , m <sup>2</sup> )                                 | —          | 5.34        | 53.73       | 4.65        | 7.14        | 7.70                   |
| Transient storage exchange rate* ( $\alpha$ , s <sup>-1</sup> )                                     | —          | 0.0032      | 0.0001      | 0.0014      | 0.0017      | 0.0024                 |
| Uptake half-saturation coefficient in channel‡ ( $k_{c1/2}$ , µg N L <sup>-1</sup> )                | —          | 25.2        | 7.6         | 15.3        | 19.2        | 21.3                   |
| Maximum uptake flux in channel‡ ( $U_{cmax}$ , µg N m <sup>-2</sup> s <sup>-1</sup> )               | —          | 16.69       | 1.41        | 4.41        | 1.42        | 9.57                   |
| Uptake half-saturation coefficient in transient storage‡ ( $k_{s1/2}$ , µg N L <sup>-1</sup> )      | —          | 23.8        | 5.0         | 14.2        | 15.2        | 19.1                   |
| Maximum uptake flux in transient storage‡ ( $U_{smax}$ , µg N m <sup>-3</sup> s <sup>-1</sup> )     | —          | 34.56       | 1.00        | 115.20      | 8.89        | 34.70                  |
| Areal nutrient uptake by uptake in channel ( $U$ , µg N m <sup>-2</sup> s <sup>-1</sup> )           | —          | 2.77        | 0.56        | 1.09        | 0.29        | 1.67                   |
| Areal nutrient uptake by uptake in transient storage ( $U$ , µg N m <sup>-2</sup> s <sup>-1</sup> ) | —          | 1.81        | 0.06        | 1.18        | 0.32        | 1.18                   |

\*Parameter values were estimated by OTIS-P.

†Full reach velocity was determined as 2610 m divided by CI travel time, 103.8 min. Cross-section area was the product of 41 m width and 0.488 m depth.

‡Parameter values were estimated by our stream model.

$$U_{cmax} = \frac{U}{C_0} (C_0 + k_{c1/2})$$

or

$$U_{smax} = \frac{U}{C_0} (C_0 + k_{s1/2}) \frac{A}{A_s} \frac{1}{z}$$

(4)

We used nominal  $k_{c1/2}$  and  $k_{s1/2}$  of 15 µg N L<sup>-1</sup> (Payn et al. 2005), which gave nominal  $U_{cmax}$  of 2.05 µg N m<sup>-2</sup> s<sup>-1</sup> and  $U_{smax}$  of 10.89 µg N m<sup>-3</sup> s<sup>-1</sup>. For our last sensitivity analysis (nutrient uptake in both channel and storage), the areal uptake of 0.51 µg N m<sup>-2</sup> s<sup>-1</sup> was the sum of uptake in both channel and storage. Assuming both  $k_{c1/2}$  and  $k_{s1/2}$  are equal, we approximated both  $U_{cmax}$  and  $U_{smax}$  as

$$U_{c_{\max}} = \frac{\gamma U}{C_0} (C_0 + k_{c1/2})$$

and (5)

$$U_{s_{\max}} = \frac{(1-\gamma)U}{C_0} (C_0 + k_{s1/2}) \frac{A}{A_s} \frac{1}{z}$$

where  $\gamma$  is the proportion of areal nutrient uptake by uptake in the stream channel.

### Model parameters for nutrient uptake estimation in the Snake River

We estimated ambient nutrient uptake in the Snake River using our model (Eq. 1 and 2) under an assumption of the Monod kinetics uptake by fitting our simulations to the results presented by Tank et al. (2008). We used the four sub-reach hydrogeomorphological estimates of the Snake River for uptake estimation (Table 2).

### Numerical methods

To simulate nitrogen uptake through time and along downstream distance, we used the fractional steps numerical method (Yanenko 1971) to solve the partial differential equations (Eq. 1 and 2). This method was originally used to simplify a multi-dimensional system into a sum of one-dimensional subsystems. Later, it was used to partition a complicated system with many processes into several subsystems with single process, where one was nested within a following one (Tsai et al. 2001; Ropp and Shadid 2005; Ropp and Shadid 2009). Ropp and Shadid (2005, 2009) and Witek et al. (2008) used the fractional steps method for advection-diffusion-reaction systems. Based on fractional steps, the first equation of the model (Eq. 1) was partitioned into three subsystems.

$$\frac{\partial C_1}{\partial t} = -\frac{Q}{A} \frac{\partial C_1}{\partial x} \quad (6)$$

$$\frac{\partial C_2}{\partial t} = \frac{1}{A} \frac{\partial}{\partial x} \left( AD \frac{\partial C_2}{\partial x} \right) \quad (7)$$

$$\frac{\partial C_3}{\partial t} = \alpha(C_3 - C_s) - U_c \quad (8)$$

where  $C_1 = C$ ,  $C_2$  is the integration of  $C_1$ , and  $C_3$  is the integration of  $C_2$ .

We used the Lagrangian approach to solve the advection Eq. 6 and substituted the solution into the dispersion Eq. 7. Using a Eulerian method with 0.01-m spatial scale and 1-s temporal scale, we numerically solved Eqs. 7 and 8 in order. This numerical solution of the model was coded in JAVA and simulated with parallel processing on a computer with a dual core processor. The numerical solution technique by the frac-

tional steps method was compared with OTIS results using an example provided in the OTIS documentation (Runkel 1998). Numerical solutions from our model and OTIS were mostly identical, except for some very small differences (mean square difference was 0.013 when we compared both numerical solutions), which may be attributed to the different numerical techniques.

### Sensitivity analysis

The model was used to simulate a series of pulse nitrogen additions under different hydrogeomorphological conditions and Monod kinetics uptake parameter values. The release point was at 0 m, and there were four downstream sampling sites (1330, 1430, 1750, and 2610 m) to monitor the downstream response. Nutrient was released at time zero. The downstream movement of the nutrient pulse was simulated over 30 h. We then calculated spiraling metrics ( $S_w$  and  $U$ , Newbold et al. 1982; Stream Solute Workshop 1990; Webster and Valett 2006) according to the TPNA technique as if our simulation was a field experiment. By measuring mass loss of the nutrient pulse as it moved downstream, the longitudinal uptake rate ( $k_x$ ) was calculated as the slope of the logarithmic transformed ratio of the remaining nutrient mass to conservative tracer mass over distance. Uptake length was calculated as the inverse of the longitudinal uptake rate ( $k_x$ ), and areal uptake was calculated as  $U = k_x v z C_0$  (Webster and Valett 2006). We compared the uptake length and areal uptake by the TPNA technique with the expected uptake length of 2000 m and areal uptake of  $0.51 \mu\text{g N m}^{-2} \text{s}^{-1}$  in our simulated large river.

The half-saturation coefficient of the Monod kinetics equation was manipulated from 5 to  $500 \mu\text{g N L}^{-1}$  to explore sensitivity of the TPNA technique to different uptake saturation levels. Payn et al. (2005) reported that half-saturation coefficient for nitrogen ranged from 6 to  $32 \mu\text{g N L}^{-1}$  and Dodds et al. (2002) gave a wider range from 1.4 to  $210 \mu\text{g N L}^{-1}$ . We chose half-saturation coefficients up to  $500 \mu\text{g N L}^{-1}$  to determine whether uptake estimates at high uptake saturation levels would converge to the uptake estimate under first-order kinetics assumption. Three hydrogeomorphological parameters ( $v$ ,  $\alpha$ , and  $A_s$ ) were also manipulated independently with three uptake saturation levels while all other hydrogeomorphological parameters were unchanged. The three uptake saturation levels were based on the half-saturation coefficient values of 5, 15, and  $50 \mu\text{g N L}^{-1}$ . The areal uptake flux ( $U$ ) at the ambient nutrient concentration was unchanged for all simulations. That is, when we changed  $k_{c1/2}$ ,  $U_{c_{\max}}$  was changed accordingly (Eq. 4), so that at  $k_{c1/2} = 5 \mu\text{g N L}^{-1}$ ,  $U_{c_{\max}} = 1.02 \mu\text{g N m}^{-2} \text{s}^{-1}$  (low uptake saturation level), at  $k_{c1/2} = 15 \mu\text{g N L}^{-1}$ ,  $U_{c_{\max}} = 2.05 \mu\text{g N m}^{-2} \text{s}^{-1}$  (medium uptake saturation level), and at  $k_{c1/2} = 50 \mu\text{g N L}^{-1}$ ,  $U_{c_{\max}} = 5.63 \mu\text{g N m}^{-2} \text{s}^{-1}$  (high uptake saturation level).

For the first four sensitivity analyses, nutrient uptake in the stream was solely in the stream channel or solely in transient storage. We ran simulations for both uptake scenarios and found that the results were similar, having the same patterns.

Hence, we only show the results for uptake in the stream channel. For our last sensitivity analysis (nutrient uptake in both channel and storage), the areal uptake as the sum of uptake in both channel and storage was unchanged while the combinations of uptake in channel and storage were manipulated.

### Assessment

Our study is based on the assumption of Monod kinetics nutrient uptake. Many studies (e.g., Dodds et al. 2002; Mulholland et al. 2002; Payn et al. 2005; Earl et al. 2006) suggested that nutrient uptake could be saturated at high nutrient concentrations, even in large rivers (Mulholland et al. 2008). However, parameters (half-saturation coefficient and maximum nutrient uptake) of Monod kinetics are difficult to measure in a stream because it requires many nutrient uptake measures at different nutrient concentration levels (including highly saturated nutrient concentration levels) to characterize the Monod kinetic uptake curve. Furthermore, the effort needed to use the constant nutrient addition technique for nutrient uptake measures at many different nutrient concentration levels in a single stream makes it nearly impractical. Consequently, nutrient uptake measures using the constant nutrient addition technique have not aimed to find the Monod kinetics uptake curve but to estimate nutrient uptake at ambient nutrient concentration by using small nutrient enrichments relative to the ambient nutrient concentration.

The PNA technique, on the other hand, can lead to a large enrichment relative to ambient conditions. Therefore, nutrient saturation is a concern. Powers et al. (2009) tested the TPNA technique under an assumption of first-order nutrient uptake kinetics. As an extension of that study, we tested the TPNA technique under the Monod kinetics nutrient uptake assumption. Manipulation of half-saturation coefficient from low to high values gave us information on how the TPNA technique performed in various uptake saturation levels and whether uptake estimates at very high saturation level agreed with first-order kinetics.

We manipulated velocity, channel-storage exchange rate, and cross-sectional storage area because they affect the degree of spread of the nutrient pulse as it moves downstream, which further influences the Monod kinetics uptake. To investigate whether these multiple factors influence the TPNA technique and whether these effects are different at various uptake saturation levels, we manipulated velocity, channel-storage exchange rate, and cross-sectional storage area at three different uptake saturation levels. Through the manipulation of these three parameters, we evaluated the sensitivity of the TPNA technique to the multiple effects of hydrogeomorphological factors and the interactions between those factors and the uptake saturation levels. Although the longitudinal dispersion coefficient in general should change the degree of spread of a solute pulse, we did not manipulate the longitudinal dispersion coefficient in the sensitivity analysis because our estimated longitudinal dispersion coefficient was low, and we would not expect signifi-

cant influence of the longitudinal dispersion coefficient when transient storage exchange is also occurring.

Last, we simulated a pulse nutrient addition and calculated nutrient uptake using the TPNA technique in a large river that had both channel and transient storage zone Monod kinetics uptake. Total uptake was fixed as  $0.51 \mu\text{g N m}^{-2} \text{ s}^{-1}$  at ambient condition. We investigated possible combinations of channel and storage uptake at which the TPNA technique would yield reliable uptake estimates.

### Monod kinetics nutrient uptake parameter manipulation

To test whether the TPNA technique was sensitive to uptake saturation levels, we kept areal uptake,  $0.51 \mu\text{g N m}^{-2} \text{ s}^{-1}$ , unchanged, while we varied  $k_{c1/2}$  from  $5 \mu\text{g N L}^{-1}$  to  $500 \mu\text{g N L}^{-1}$ .  $U_{\text{max}}$  was changed correspondingly using Eq. 4. The uptake-estimate curve in Fig. 1 represents the uptake estimates by the TPNA technique at different uptake saturation levels and the

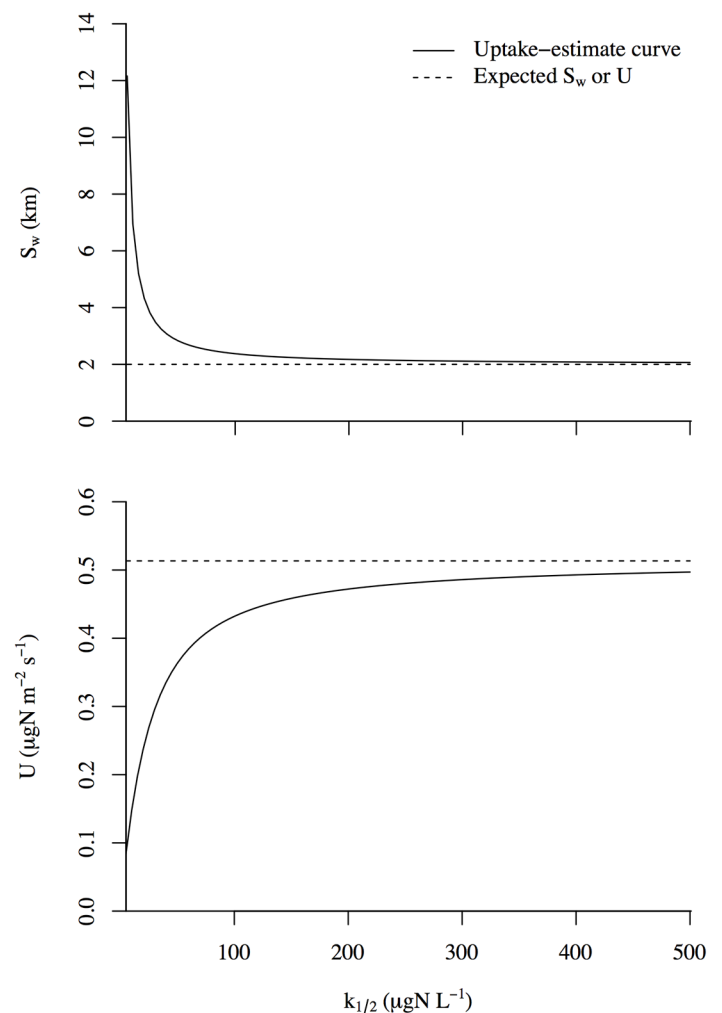


**Fig. 1.** Sensitivity of the TPNA technique to the Monod kinetics parameters. Uptake-estimate curve represents the uptake estimates by the TNPA technique in a simulated large river at different uptake saturation levels. The expected  $S_w$  and  $U$  are the spiraling metrics at ambient conditions in our simulation.

ambient uptake is the dashed line (expected  $S_w$  or  $U$ ). The difference between the uptake-estimate curve and ambient uptake was high at low uptake saturation level and gradually decreased as the uptake saturation level became higher (Fig. 1). Uptake estimates by the TPNA technique asymptotically approached ambient uptake at very high uptake saturation levels. This result also suggested that uptake estimates by the TPNA technique under first-order and Monod kinetics assumptions converge when the uptake saturation level is very high.

### Velocity manipulation

We simulated pulse nutrient additions at velocities ranging from 0.1 to 1.4  $\text{m s}^{-1}$  at each of the three uptake saturation levels. Discharge ( $Q = vA$ ) and uptake flux ( $U = k_x v z C_0$ ) at ambient nutrient concentration were held constant when we changed the current velocity. That is, when we changed velocity ( $v$ ), cross-sectional area ( $A$ ), and the longitudinal uptake rate ( $k_x$ ) were changed accordingly to maintain the same discharge and areal uptake flux. Since water depth ( $z$ ) could affect uptake ( $U$ ), we changed the channel width ( $w$ ) and held depth constant when we corrected cross-sectional area for velocity. When cross-sectional area changed, cross-sectional transient storage area ( $A_s$ ) was also corrected to keep the ratio  $A_s A^{-1}$  unchanged.

All three uptake-estimate curves showed similar patterns, i.e., the difference between the uptake-estimate curve and ambient uptake was small at low velocities and large at high velocities (Fig. 2). There were also variations among the uptake-estimate curves. All three uptake-estimate curves had similar values at low velocity, which were close to ambient uptake. As velocity increased, uptakes-estimate curves with lower uptake saturation deviated more from ambient uptake than the ones with higher uptake saturation (Fig. 2). Results from the sensitivity analysis suggested that velocity affects the degree of spread of the nutrient pulse and further influences nutrient uptake kinetics.

### Cross-sectional storage area manipulation

The cross-sectional transient storage area,  $A_s$ , was changed from 2.0 to 40.0  $\text{m}^2$ , i.e.,  $A_s/(A_s + A)$  ranged from 0.09 to 0.67. All three uptake-estimate curves at different uptake saturation levels showed similar patterns, i.e., the difference between the uptake-estimate curve and ambient uptake was large at low  $A_s/(A_s + A)$  and small at high  $A_s/(A_s + A)$  (Fig. 3). Variations among uptake-estimate curves were also great at low  $A_s/(A_s + A)$ . Manipulation of  $A_s$  suggested that the size of transient storage effected the spread of the nutrient pulse. Greater  $A_s$  lead to greater spread of the nutrient pulse and less difference between the TPNA estimate and ambient uptake.

### Channel-storage exchange rate manipulation

Transient storage and main channel cross-sectional areas were fixed when we manipulated the channel-storage exchange rate,  $\alpha$ . By changing  $\alpha$  from 0.0002 to 0.003  $\text{s}^{-1}$ , we controlled the average residence time of a nutrient molecule in the storage zone. The metric  $f_{\text{med}}$  (Runkel 2002), which measures the fraction of the median travel time due to transient storage, was 0.19

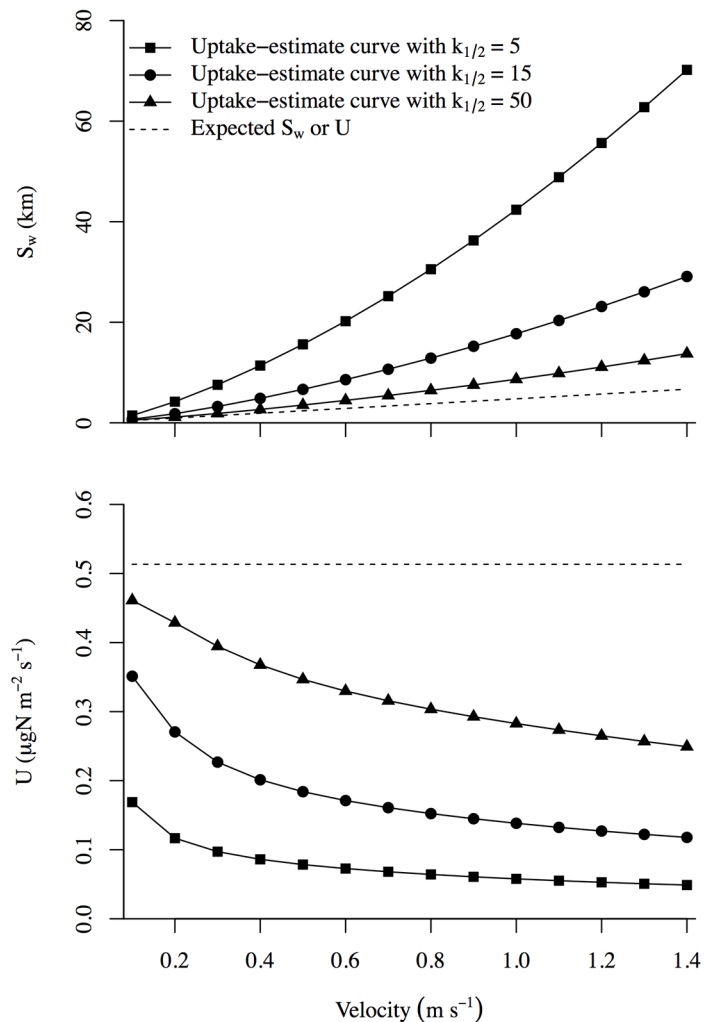


**Fig. 2.** Sensitivity of the TPNA technique to velocity. Uptake-estimate curves represent the uptake estimates by the TPNA technique in a simulated large river at different velocities. The expected  $S_w$  and  $U$  are the spiraling metrics at ambient conditions in our simulation.

at the lowest  $\alpha$  (0.0002  $\text{s}^{-1}$ ), but as we increased  $\alpha$  to 0.0006  $\text{s}^{-1}$ ,  $f_{\text{med}}$  approached a constant fraction, 0.32.

To illustrate the influence of exchange rate on a solute pulse, we plotted the conservative tracer pulse passing the last station (2610 m) at different exchange rates (Fig. 4). At a low exchange rate (0.0002  $\text{s}^{-1}$ ), more than half of the tracer mass passed the 2610-m station in a very short period (Fig. 4), suggesting low degree of spread. At a medium-low exchange rate (0.0006  $\text{s}^{-1}$ ), the tracer concentration gradually increased and flattened, implying relatively higher degree of spread. For the tracer pulse with a high exchange rate (0.003  $\text{s}^{-1}$ ), most of the tracer went into the storage zone but quickly returned, indicated by the delay in time and the shape of the pulse. Although the tracer easily spread under the high exchange rate, the short storage residence time reduced the effective spread.

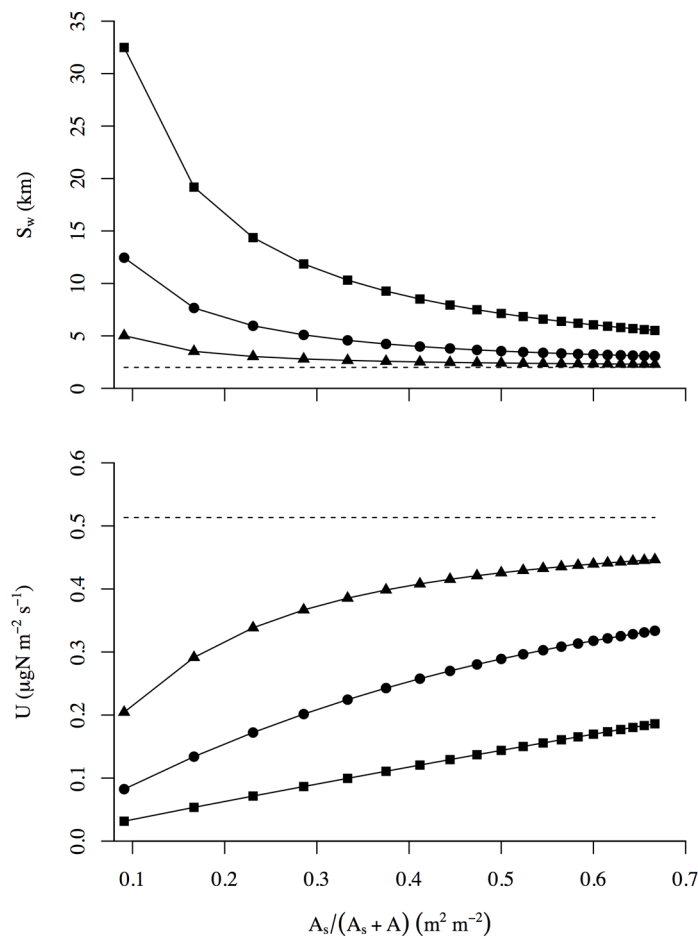


**Fig. 3.** Sensitivity of the TPNA technique to cross-sectional transient storage area. Symbols are the same as Fig. 2. Uptake-estimate curves represent the uptake estimates by the TNPA technique in a simulated large river at different  $A_s/(A_s+A)$ . The expected  $S_w$  and  $U$  are the spiraling metrics at ambient conditions in our simulation.

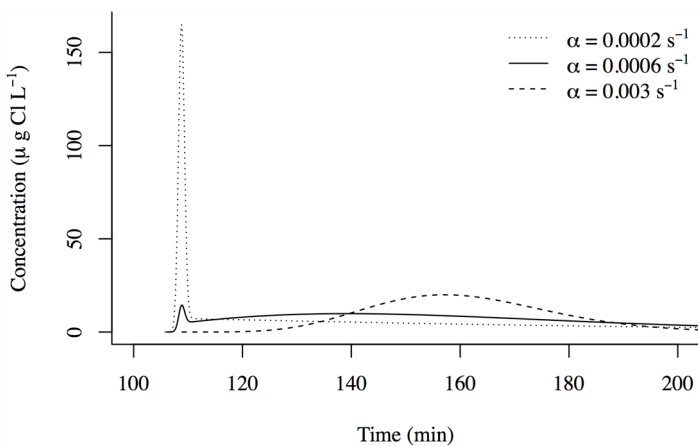


**Fig. 4.** Simulated conservative tracer slugs at 2610 m at different channel-storage exchange rates.

Our sensitivity analysis showed that all three uptake-estimate curves at different uptake saturation levels had similar patterns. Differences between uptake-estimate curves and ambient uptake declined as exchange rate increased at medium-low exchange rate and then gradually increased. Differences between uptake-estimate curves and ambient uptake were higher with low uptake saturation level and lower with high uptake saturation level, which agreed with the results from Monod kinetic sensitivity analysis. Variations among uptake-estimate curves in this analysis of exchange rate were not as great as those in the sensitivity analysis of velocity and cross-sectional transient storage area. Results suggested that exchange rate could increase or decrease the degree of spread of the nutrient pulse (Fig. 5) but had significant influence on shifting the TPNA technique estimates when the exchange rate was very low ( $0.0002 - 0.0006 \text{ s}^{-1}$ ) or when the uptake saturation level was low.

In general, sensitivity of the TPNA technique to physical characteristics of the river was related to the spread of the nutri-

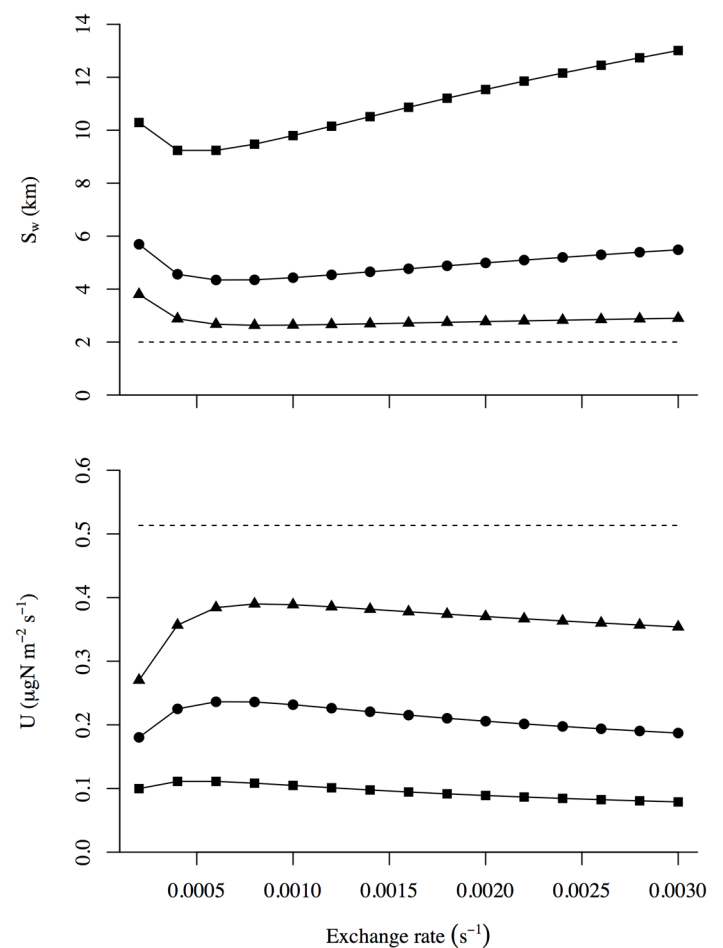


**Fig. 5.** Sensitivity of the TPNA technique to channel-storage exchange rate. Symbols are the same as Fig. 2. Uptake-estimate curves represent the uptake estimates by the TNPA technique in a simulated large river at different channel-storage exchange rate. The expected  $S_w$  and  $U$  are the spiraling metrics at ambient conditions in our simulation.

ent pulse. Another way to increase the spread and thus reduce the peak nutrient concentration and the extent of nutrient saturation would be to sample further downstream. To evaluate the impact of sampling distance on nutrient uptake estimation, we doubled and tripled the nominal sampling distances, and estimated nutrient uptake using the TPNA technique at the doubled and tripled distances, respectively. Estimated uptake ( $U$ ) by the TPNA technique was  $0.20 \mu\text{g N m}^{-2} \text{s}^{-1}$  at the nominal sampling distances,  $0.26 \mu\text{g N m}^{-2} \text{s}^{-1}$  at the doubled sampling distances, and  $0.31 \mu\text{g N m}^{-2} \text{s}^{-1}$  at the tripled sampling distances, and the expected uptake was  $0.51 \mu\text{g N m}^{-2} \text{s}^{-1}$ .

#### Nutrient uptake in both the stream channel and in transient storage

In this simulation, we kept areal uptake ( $0.51 \mu\text{g N m}^{-2} \text{s}^{-1}$ ) unchanged but manipulated the combination of Monod kinetics nutrient uptake in the stream channel and transient storage. We used the nominal value of  $k_{1/2}$  ( $15 \mu\text{g N L}^{-1}$ ). The calculated areal uptake by the TPNA technique did not change significantly at different nutrient uptake combinations in channel and storage (Fig. 6) but was lower ( $0.19 \mu\text{g N m}^{-2} \text{s}^{-1}$ ) than ambient uptake, regardless whether uptake was in the channel or storage or any combination of the two. Perhaps uptake in the channel or transient storage affected the timing of ammonium uptake but did not affect the mass of ammonium removed and therefore did not affect the estimate of uptake by the TPNA technique.

#### Discussion

Our results were different from those of Powers et al. (2009), in which first-order uptake kinetics was assumed. When nutrient uptake follows first-order kinetics, nutrient uptake is linearly proportional to the available nutrient concentration. Total nutrient mass loss is the product of the uptake rate and total nutrient mass, regardless of any hydrogeomorphological influences on the degree of spread of the nutrient pulse. Nutrient uptake measures that rely on nutrient mass loss to calculate spiraling metrics should give reasonable uptake estimates if there is first-order uptake, but Powers et al. (2009) also noted that the TPNA technique might yield different results if uptake was nonlinear, as we have shown in this study. When nutrient uptake follows Monod kinetics, nutrient uptake increases with a decreasing rate as nutrient concentration increases, uptake is less than the first-order uptake kinetics, and this uptake difference increases at higher nutrient concentration. Nutrient mass loss at downstream stations, hence, does not represent nutrient uptake at ambient nutrient concentration. Furthermore, hydrogeomorphological parameters (e.g., velocity, cross-sectional storage area, and channel-storage exchange rate) also change the degree of spread of the nutrient pulse and further affect uptake both spatially and temporally.

Results from our analyses of the TPNA technique would be restricted by two conditions: first, nutrient uptake in the experimental stream follows Monod kinetics; second, concentrations during the nutrient pulse approach nutrient saturation

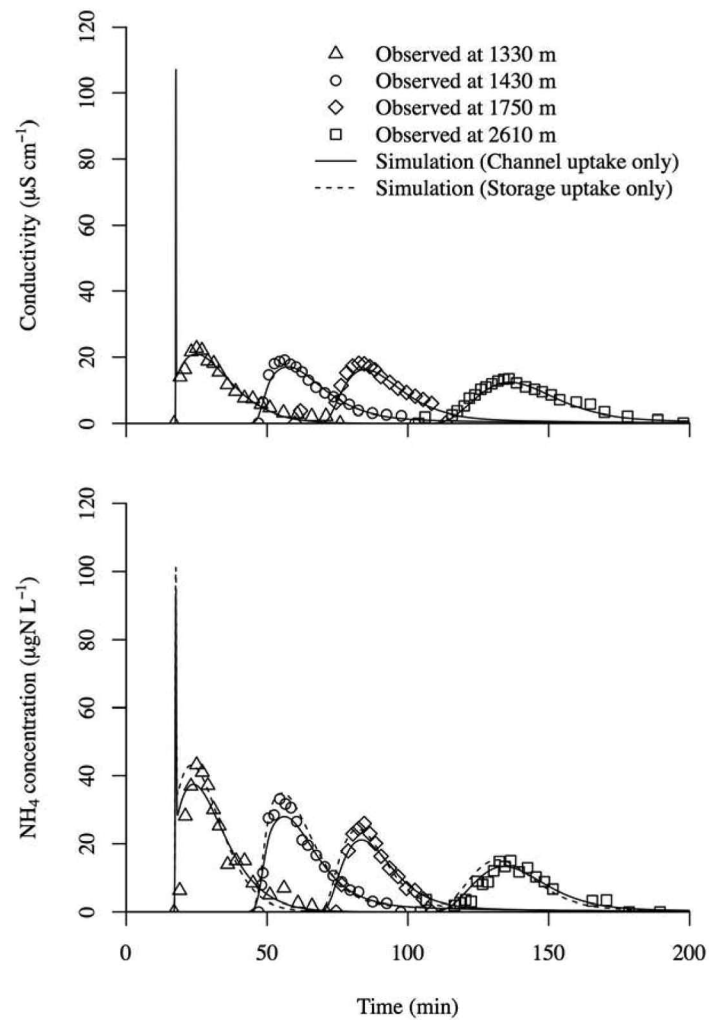


**Fig. 6.** Simulated and observed conductivity and  $\text{NH}_4^+$  concentration at downstream stations in the Snake River. For conductivity fitting,  $r^2 = 0.95$ ; for  $\text{NH}_4^+$  concentration using channel Monod kinetics uptake,  $r^2 = 0.86$ ; and for  $\text{NH}_4^+$  concentration using storage Monod kinetics uptake,  $r^2 = 0.89$ .

tion. For stream study reaches that have high lateral inflow or groundwater input, the nutrient pulse would be diluted as it travels downstream, which may reduce the chance of nutrient saturation. Further research would be needed to completely understand the effects of dilution by lateral inflow or groundwater input to the TPNA technique.

#### Recommendation

Runkel (2007) recommended the use of time-series data and the quantification of a dynamic model to evaluate solute transport and uptake in streams. We extend his recommendation by emphasizing the need to use nonlinear uptake, such as Monod kinetics. To exemplify this approach, we used the ammonium data for the Snake River (Tank et al. 2008). We partitioned the 2610-m full reach into four sub-reaches (0–1330 m, 1330–1430 m, 1430–1750 m, and 1750–2610 m)

based on the sampling sites and used the OTIS-P model (Runkel 1998) to estimate the hydrogeomorphological parameters for each reach (Table 2 and Fig. 6 upper). Monod kinetic parameters (Eq. 3) were estimated by fitting the simulated ammonium concentration to the data from the Snake River in each sub-reach. Two metrics, Absolute Median Error (AME) and Mean Absolute Error (MAE), were used to evaluate the goodness of fit of our model. We tested different combinations of  $k_{1/2}$  (ranging from 5 to 26) and  $U_{\max}$  (0.07 to 19.14), and selected the Monod kinetic parameters that yielded the smallest AME and MAE values. Using Eq. 3, we calculated areal uptake at ambient ammonium concentration using the fitted Monod kinetic parameters in each sub-reach (Table 2). Since we do not know the proportions of uptake in the stream channel and in transient storage, we made two uptake estimates: uptake in the stream channel only and uptake in transient storage only (Fig. 6 lower). The model using storage uptake performed better when fitting the observed peaks while the model using channel uptake performed better when fitting the observed falling limbs at the first three stations (1330 m, 1430 m, and 1750 m). At the last station (2610 m), the model using channel uptake fit the observed better than the model using storage uptake. Both channel and storage uptake analyses showed that nutrient areal uptake in the first sub-reach was the highest, followed by the third, second, and fourth sub-reaches (Table 2). Our estimated half-saturation coefficient was lower than the peak enrichment of ammonium in each sub-reach, which further supported our assumption that nutrient saturation likely occurred in the Snake River during the nutrient pulse injection by Tank et al. (2008). We calculated the full reach areal uptake as the weighted average of areal uptake in the four sub-reaches. The full reach areal uptake was  $1.67 \mu\text{g N m}^{-2} \text{s}^{-1}$  (uptake length 616 m, uptake in channel only) and  $1.18 \mu\text{g N m}^{-2} \text{s}^{-1}$  (uptake length 873 m, uptake in storage only), which are both more than double the estimated uptake calculated by Tank et al. (2008).

The difference between our uptake estimate and the estimates by Tank et al. (2008) can be attributed to different nutrient uptake functional responses: Monod kinetics and first-order kinetics. Without further investigations, the two estimates could be thought as the lower and upper bounds of estimated ammonium uptake in the Snake River. In general, nutrient uptake saturation levels are unknown in large rivers, but our results suggest that the pulse addition resulted in ammonium concentration that approached, or in some cases, exceeded saturation resulting in an underestimate of ambient ammonium uptake.

One limitation of our modeling approach is our assumption of nutrient-independent mineralization from the biofilm to the water column over the period of the experiment. This may have led to an underestimate of biological nutrient uptake. For example, in our model, in-stream nutrient mineralization was a constant nutrient flux to the stream, independent of nutrient concentration. The modeled stream reach

was assumed to be at steady state before the pulse release of nutrient, i.e., nutrient mineralization was equal to  $U$  at the ambient nutrient concentration and net nutrient uptake was zero. As the pulse of nutrient was released to our modeled stream reach, it elevated the in-stream nutrient concentration above ambient and led to an increase in nutrient uptake but no effect on nutrient mineralization. When we used the model simulation to fit the observed data with a constant mineralization flux, the uptake value we estimated may have been smaller than what it should have been. If we were to include variable mineralization in our model, it would further elevate our estimate of ammonium uptake.

In conclusion, the TPNA technique is sensitive to both hydrogeomorphology and Monod kinetic parameters. It may be possible to use the PNA technique to quantify a fully dynamic model and obtain useful information about stream nutrient dynamics in a large river. In various studies, models have been used to estimate the retention of nutrients, particularly nitrogen, by rivers (Alexander et al. 2000; Peterson et al. 2001; Wollheim et al. 2006; Mulholland et al. 2008). These studies have generally emphasized the role of small streams in retaining or removing nutrient from the river network and noted the need for data on large rivers, though Wollheim et al. (2006) showed high potential of large rivers for nutrient retention. Empirical measurements in large rivers are costly, time-consuming, and daunting, but our results suggest that thorough analysis of the data may provide useful estimates of river processes. Covino and others (2010a, 2010b) suggested an alternative analysis of the breakthrough curve generated by pulse addition, which may be more useful than the method analyzed in this study. However, sensitivity analyses are needed to verify this alternative PNA technique.

## References

- Alexander, R. B., R. A. Smith, and G. E. Schwarz. 2000. Effect of stream channel size on the delivery of nitrogen to the Gulf of Mexico. *Nature* 403:758-761 [[doi:10.1038/35001562](https://doi.org/10.1038/35001562)].
- Bencala, K. E., and R. A. Walters. 1983. Simulation of solute transport in a mountain pool-and-riffle stream: a transient storage model. *Water Resour. Res.* 19:718-724 [[doi:10.1029/WR019i003p00718](https://doi.org/10.1029/WR019i003p00718)].
- Bothwell, M. L. 1989. Phosphorus limited growth dynamics of lotic periphytic diatom communities - areal biomass and cellular growth-rate responses. *Can. J. Fish. Aquat. Sci.* 46:1293-1301 [[doi:10.1139/f89-166](https://doi.org/10.1139/f89-166)].
- Claessens, L., and C. L. Tague. 2009. Transport-based method for estimating in-stream nitrogen uptake at ambient concentration from nutrient addition experiments. *Limnol. Oceanogr. Methods* 7:811-822 [[doi:10.4319/lom.2009.7.811](https://doi.org/10.4319/lom.2009.7.811)].
- Covino, T. P., B. L. McGlynn, and M. Baker. 2010a. Separating physical and biological nutrient retention and quantifying uptake kinetics from ambient to saturation in successive mountain stream reaches. *J. Geophys. Res.* 115:G04010 [[doi:10.1029/2009JG001263](https://doi.org/10.1029/2009JG001263)].

- , ———, and R. A. McNamara. 2010b. Tracer Additions for Spiraling Curve Characterization (TASCC): Quantifying stream nutrient uptake kinetics from ambient to saturation. *Limnol. Oceanogr. Methods* 8:484-498 [doi:10.4319/lom.2010.8.484].
- Dodds, W. K., and others. 2002. N uptake as a function of concentration in streams. *J. North Am. Benthol. Soc.* 21:206-220 [doi:10.2307/1468410].
- Earl, S. R., H. M. Valett, and J. R. Webster. 2006. Nitrogen saturation in stream ecosystems. *Ecology* 87:3140-3151 [doi:10.1890/0012-9658(2006)87[3140:NSISE]2.0.CO;2].
- Elwood, J. W., J. D. Newbold, R. V. O'Neill, R. W. Stark, and P. T. Singley. 1981. The role of microbes associated with organic and inorganic substrates in phosphorus spiraling in a woodland stream. *Verh. Internat. Verein. Theor. Angew. Limnol.* 21:850-856.
- Kemp, M. J., and W. K. Dodds. 2002. The influence of ammonium, nitrate, and dissolved oxygen concentrations on uptake, nitrification, and denitrification rates associated with prairie stream substrata. *Limnol. Oceanogr.* 47:1380-1393 [doi:10.4319/lo.2002.47.5.1380].
- Martin, L. A., P. J. Mulholland, J. R. Webster, and H. M. Valett. 2001. Denitrification potential in sediments of headwater streams in the southern Appalachian Mountains, USA. *J. North Am. Benthol. Soc.* 20:505-519 [doi:10.2307/1468084].
- Meals, D., and others. 1999. Retention of spike additions of soluble phosphorus in a northern eutrophic stream. *J. North Am. Benthol. Soc.* 18(2):185-198 [doi:10.2307/1468460].
- Mulholland, P. J., and others. 2002. Can uptake length in streams be determined by nutrient addition experiments? Results from an interbiome comparison study. *J. North Am. Benthol. Soc.* 21:544-560 [doi:10.2307/1468429].
- , and others. 2008. Stream denitrification across biomes and its response to anthropogenic nitrate loading. *Nature* 452:202-U246 [doi:10.1038/nature06686].
- Newbold, J. D., J. W. Elwood, R. V. O'Neill, and W. VanWinkle. 1981. Measuring nutrient spiraling in streams. *Can. J. Fish. Aquat. Sci.* 38:860-863 [doi:10.1139/f81-114].
- , R. O'Neill, J. Elwood, and W. Van Winkle. 1982. Nutrient spiraling in streams: implications for nutrient limitation and invertebrate activity. *Amer. Natural.* 120:628-652 [doi:10.1086/284017].
- Payn, R. A., J. R. Webster, P. J. Mulholland, H. M. Valett, and W. K. Dodds. 2005. Estimation of stream nutrient uptake from nutrient addition experiments. *Limnol. Oceanogr. Methods* 3:174-182 [doi:10.4319/lom.2005.3.174].
- Peterson, B. J., and others. 2001. Control of nitrogen export from watersheds by headwater streams. *Science* 292:86-90 [doi:10.1126/science.1056874].
- Powers, S. M., E. H. Stanley, and N. R. Lottig. 2009. Quantifying phosphorus uptake using pulse and steady-state approaches in streams. *Limnol. Oceanogr. Methods* 7:498-508 [doi:10.4319/lom.2009.7.498].
- Ropp, D. L., and J. N. Shadid. 2005. Stability of operator splitting methods for systems with indefinite operators: reaction-diffusion systems. *J. Comput. Phys.* 203:449-466 [doi:10.1016/j.jcp.2004.09.004].
- , and ———. 2009. Stability of operator splitting methods for systems with indefinite operators: Advection-diffusion-reaction systems. *J. Comput. Phys.* 228:3508-3516 [doi:10.1016/j.jcp.2009.02.001].
- Rosemond, A. D., P. J. Mulholland, and J. W. Elwood. 1993. Top-down and bottom-up control of stream periphyton—effects of nutrients and herbivores. *Ecology* 74:1264-1280 [doi:10.2307/1940495].
- Runkel, R. L. 1998. One-Dimensional Transport with Inflow and Storage (OTIS): A solute transport model for streams and rivers. U.S. Geological Survey Water-Resources Investigations Report 98:73.
- . 2002. A new metric for determining the importance of transient storage. *J. North Am. Benthol. Soc.* 21:529-543 [doi:10.2307/1468428].
- . 2007. Toward a transport-based analysis of nutrient spiraling and uptake in streams. *Limnol. Oceanogr. Methods* 5:50-62 [doi:10.4319/lom.2007.5.50].
- Stream Solute Workshop. 1990. Solute dynamics in streams. *J. North Am. Benthol. Soc.* 9:95-119 [doi:10.2307/1467445].
- Tank, J. L., E. J. Rosi-Marshall, M. A. Baker, and R. O. Hall. 2008. Are rivers just big streams? A pulse method to quantify nitrogen demand in a large river. *Ecology* 89:2935-2945 [doi:10.1890/07-1315.1].
- Tsai, T., J. Yang, and L. Huang. 2001. An accurate integral-based scheme for advection-diffusion equation. *Commun. Numer. Meth. En.* 17:701-713 [doi:10.1002/cnm.442].
- Webster, J. R., and B. C. Patten. 1979. Effects of watershed perturbation on stream potassium and calcium dynamics. *Ecol. Monogr.* 49:51-72 [doi:10.2307/1942572].
- , and H. M. Valett. 2006. Solute dynamics, p. 169-185. *In* F. R. Hauer and G. A. Lamberti [eds.], *Methods in stream ecology*. Academic Press.
- Witek, M., J. Teixeira, and P. Flatau. 2008. On stable and explicit numerical methods for the advection-diffusion equation. *Math. Comput. Simulat.* 79:561-570 [doi:10.1016/j.matcom.2008.03.001].
- Wollheim, W. M., C. J. Vorosmarty, B. J. Peterson, S. P. Seitzinger, and C. S. Hopkins. 2006. Relationship between river size and nutrient removal. *Geophys. Res. Lett.* 33:1-4 [doi:10.1029/2006GL025845].
- Yanenko, N. N. 1971. The method of fractional steps, the solution of problems of mathematical physics in several variables (English translated by M. Holt.). Springer-Verlag.

Submitted 6 June 2011

Revised 5 June 2012

Accepted 19 June 2012